PERKIN 2

Unique reflection properties of thin films of organic soluble naphthalocyanines

Takeo Tomiyama,[a] Seiji Tai,*[,b] Mitsuo Katayose,[b] Masanobu Habiro[a] and Nobuyuki Hayashi[a]

[a] *Tsukuba Research Laboratory, Hitachi Chemical Co., Ltd., 48, Wadai, Tsukuba 300-42, Japan*

[b] *Ibaraki Research Laboratory, Hitachi Chemical Co., Ltd., 13-1, 4-Chome, Higashi-cho, Hitachi 317, Japan*

The reflection properties of a series of organic-soluble naphthalocyanines (Y_2MNcX_4 1 and $MNcX_4$ 2), in thin films have been studied: their reflection properties were quite different. The maximal reflectivity of a thin film of an example of naphthalocyanine 1 such as $(Et_3SiO)_2SiNc(SC_{10}H_{21})_4$ (1b) was over 0.5 around the near IR region, whereas an example of compound 2 such as $NiNc(Bu^t)_4$ (2a) showed broad reflection spectra below a reflectivity of 0.25 as a thin film. To explain these different reflection properties of thin films of 1 and 2, their complex dielectric constants (relative permittivities) determined from their experimentally obtained spectral data were analysed. The highly ordered J-type molecular arrangement of a thin film of 1 generated a sharp dielectric maximum with a large oscillator strength and a narrow peak width, whereas the complex and disordered molecular aggregation of a thin film of 2 induced a broad dielectric maximum. The unique differences between thin films of 1 and 2 arose from their dielectric properties.

The optical properties of organic dyes have recently attracted much attention from materials chemists because of their potential use in optical devices.[1] Especially, near IR dyes are useful for optical recording materials in optical disks since they effectively absorb the semiconductor laser light (about 800 nm).[2] Among these near IR absorbing dyes, naphthalocyanine (Nc) could be most suitable for use in optical recording materials since it has high chemical stability. In particular, organic-soluble Ncs have advantages for such applications because they are easily purified by column chromatography and/or recrystallization. Although many Ncs have been patented for use in optical recording materials, fundamental research on their spectral properties has been restricted. We have synthesized many Ncs and studied their absorption and fluorescence properties in solutions and in thin films.[3–6] From our studies on correlation of their spectral properties with their molecular structures, Ncs were classified into two types of compounds.[3] One is represented as $MNcX_4$ which shows strong aggregating tendencies, forming H-aggregates such as face-to-face dimer, trimer, tetramer, *etc.*, even in dilute solutions. Thin films of $MNcX_4$ tend to form a mixture of the H-type aggregates and a small amount of the J-type arrangement, because of their aggregating tendencies and the partial steric hindrance of four X groups.[4] The other is Y_2MNcX_4 which has monomerically pure characteristics in solution and has a relatively ordered J-type molecular arrangement in thin films due to the steric hindrance of two Y groups such as R_3SiO–.[5] The molecular structures of $MNcX_4$ 2 and Y_2MNcX_4 1 are shown in Fig. 1.

For optical recording materials, another important property is the reflectivity of the organic dye film. Although the reflectivity of organic thin films is usually low compared with that of metals or inorganic materials, some Ncs show high reflectivity. However, fundamental research into their reflection properties has never been performed so far.

Here we describe and discuss the reflection properties of Ncs in thin films by analysing their complex dielectric constants in relation to their molecular arrangement.

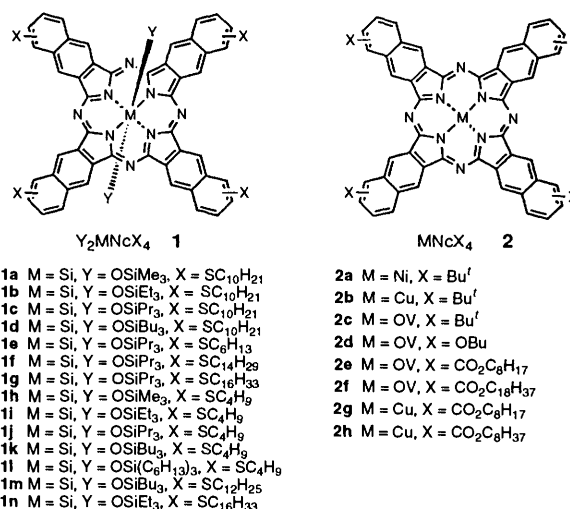

Fig. 1 Molecular structures of Y_2MNcX_4 1 and $MNcX_4$ 2

Experimental

Apparatus

The normal incident reflection and transmission spectra were measured using Hitachi U-3400 spectrophotometers. Reflectivities were corrected to absolute reflectivities using a standard Al mirror. Film thickness was measured using Sloan Dektak 3030 surface profiler. The surfaces of thin films were observed under a Nikon Microphot-FX polarization microscope.

Materials

All Ncs (1 and 2) have been synthesized previously.[3,4]

Preparation of thin solid films

Solutions of Ncs in $CHCl_3$ were dropped onto non-alkali glass plates of 1.0 mm thickness and then spin-coated using a Mikasa

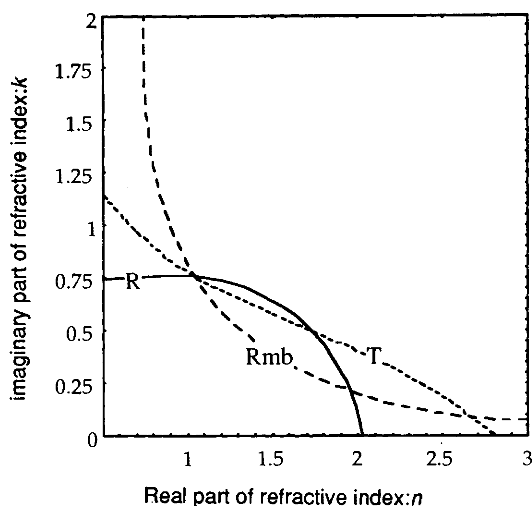

Fig. 2 Plot of three trajectories from eqns. (1)–(3) for a thin film of **1b** of 45 nm thickness at 1.588 eV (780 nm) in the n–k plane ($T = 0.617$, $R = 0.127$ and $R_{mb} = 0.686$)

1H-D2 spinner (1st, 150 rpm × 10 s; 2nd, 1000 rpm × 60 s) at 25 °C. The film thickness was controlled by varying the concentration of the Nc.

A sample for measuring the substrate incident reflectivity of a thin film on an Au layer (Rmb_{exp}) was formed by sputtering Au onto the Nc film obtained above.

Determination of the complex refractive index

In the light of complicated multiple interference phenomena between reflections from several interfaces such as air-incident reflections from air/film and film/substrate interfaces,[7] complex refractive indices ($N_2 = n - ik$) of thin films were determined from experimentally obtained substrate-incident reflectivity on the Au layer (Rmb_{exp}), air-incident transmissivity (T_{exp}) and air-incident reflectivity (R_{exp}) using eqns. (1)–(3),

$$Rmb_{cal}[n, k, N_3, N_4, d, \lambda] - Rmb_{exp} = 0 \quad (1)$$

$$T_{cal}[n, k, N_1, N_3, d, \lambda] - T_{exp} = 0 \quad (2)$$

$$R_{cal}[n, k, N_1, N_3, d, \lambda] - R_{exp} = 0 \quad (3)$$

where Rmb_{cal}, T_{cal} and R_{cal}, respectively, indicate instructions to calculate the substrate-incident reflectivity of the thin film on the Au layer, air-incident transmissivity and reflectivity of the thin film, N_1, N_3 and N_4, respectively, show complex refractive indices of air, substrate and Au, d is the thickness of the thin film, and λ is the wavelength of incident light. The Rmb_{cal}, T_{cal} and R_{cal} are given by eqns. (4)–(6), where r_{mb} and r are complex

$$Rmb_{cal} = |r_{mb}|^2 \quad (4)$$

$$T_{cal} = (N_3/N_1) \times |t|^2 \quad (5)$$

$$R_{cal} = |r|^2 \quad (6)$$

reflection coefficients of substrate-incident reflectivity of the thin film on the Au layer and air-incident reflectivity of the thin film and t is a complex transmission coefficient of air-incident transmissivity of the thin film. The r_{mb}, t and r are represented by eqns. (7)–(9), where r_{12}, r_{23}, r_{32} and r_{24} are, respectively, the

$$r_{mb} = \frac{r_{32} + r_{24}\exp(-2i\psi)}{1 + r_{32}r_{24}\exp(-2i\psi)} \quad (7)$$

$$t = \frac{t_{12}t_{23}\exp(-i\psi)}{1 + r_{12}r_{23}\exp(-2i\psi)} \quad (8)$$

$$r = \frac{r_{12} + r_{23}\exp(-2i\psi)}{1 + r_{12}r_{23}\exp(-2i\psi)} \quad (9)$$

Fresnel reflection coefficients of air/thin film, thin film/substrate, substrate/thin film and thin film/Au interfaces, t_{12} and t_{23} are, respectively, the Fresnel transmission coefficients of air/thin film and thin film/substrate interfaces, and ψ is parameter of film thickness. The r_{12}, r_{23}, t_{12}, t_{23}, r_{32}, r_{24} and ψ are shown by eqns. (10)–(16).

$$r_{12} = \frac{N_1 - N_2}{N_1 + N_2} \quad (10)$$

$$r_{23} = \frac{N_2 - N_3}{N_2 + N_3} \quad (11)$$

$$t_{12} = \frac{2N_1}{N_1 + N_2} \quad (12)$$

$$t_{23} = \frac{2N_2}{N_2 + N_3} \quad (13)$$

$$r_{32} = \frac{N_3 - N_2}{N_3 + N_2} \quad (14)$$

$$r_{24} = \frac{N_2 - N_4}{N_2 + N_4} \quad (15)$$

$$\psi = \frac{2\pi}{\lambda} N_2 d \quad (16)$$

Possible solutions (n and k) from each eqn. [(1)–(3)] were plotted as a trajectory in the n–k plane. Fig. 2 shows a typical example of three trajectories from eqns. (1)–(3) for a thin film of **1b** of 45 nm thickness at 1.588 eV (780 nm). The intersection of the three trajectories was the correct solution ($N = 1.04 - i$ 0.75). From these calculations between 1.2 and 2.5 eV, the action spectra of k and n were obtained as shown in Figs. 6 and 7.

Although several solutions were obtained from the usual R–T method using two of eqns. (1)–(3),[8] our three-trajectories method gave only a single correct solution.

Results and discussion

The air-incident transmission and reflection spectra of $(Et_3SiO)_2SiNc(SC_{10}H_{21})_4$ **1b**, a typical example of Y_2MNcX_4 **1** having two sterically hindered Y groups such as Et_3SiO–, in thin film of a 45 nm thickness are shown in Fig. 3(*a*), while those of $NiNc(Bu^t)_4$ **2a**, a typical example of $MNcX_4$ **2**, in thin film of a 43 nm thickness are depicted in Fig. 3(*b*). The surfaces of the resultant films were sufficiently flat and micro-crystals were not observed. The Q-band absorption of the **1b** film was quite intense in the near IR region and its maximal reflectivity reached 0.5 around 1.47 eV. On the other hand, the **2a** film had broad absorption bands in the visible to near IR region. The reflection spectrum of the **2a** film was also broad and the reflectivity was around 0.15. Therefore, the maximal reflectivity of the **1b** film was over three times higher than that of the **2a** film. Thin films of other compounds **1** also showed significantly large maximal reflectivity (see Fig. 11) compared with those of other compounds **2**. Consequently, the maximal reflectivity of the films of **1** was over 0.4, whereas that of the films of **2** was below 0.2.

A series of the air-incident reflection spectra of thin films **1b** and **2a** of various thicknesses around the near IR region are shown in Figs. 4 and 5, respectively. As summarized in Fig. 4, the reflection spectra of thin films of **1b** were remarkably dependent on the thickness. The maximal reflectivity was 0.4

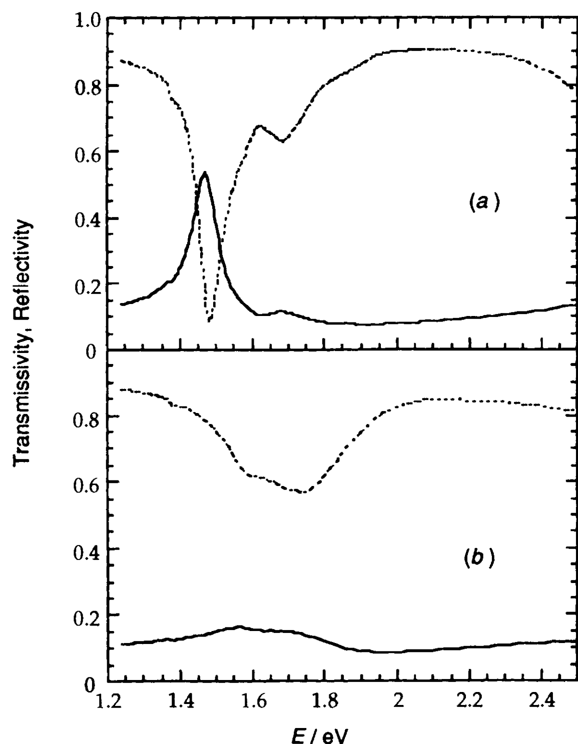

Fig. 3 Air-incident transmission (- - -) and reflection (—) spectra of thin films of **1b** [(*a*), 45 nm thickness] and **2a** [(*b*), 43 nm thickness]

even at 25 nm and reached 0.56 around 64 nm thickness. A reflection spectral hole with a large contrast and a narrow band width in the films of **1b** was observed at > 64 nm thickness. The spectral hole is unique in a thin film consisting of a single organic layer. Similar remarkable dependence of the reflection spectra of other compounds **1** on their film thicknesses was observed. On the contrary, the reflection spectra of thin films of **2a** were slightly dependent on film thickness and the maximal reflectivity was less than 0.22 as shown in Fig. 5. A spectral hole was not observed at any film thickness. Other thin films of compound **2** showed similar reflection properties.

To discuss these reflection properties of thin films of **1** and **2**, analysis of their complex dielectric constant (ε) is valuable because ε is an intrinsic physical property of any material.

The ε was determined *via* calculating the complex refractive indices (n and k) of thin films of **1b** and **2a** of 45 and 43 nm thicknesses, respectively. The complex refractive indices, n and k, were calculated by means of our three-trajectories method from the action spectra shown in Fig. 3. This method was preferable to the R–T method.[8] The calculated action spectra of the imaginary (k) and real parts (n) of the complex refractive index for the **1b** film are given in Fig. 6(*a*) and (*b*), respectively.†

† Using the k- and n-values, reflection spectra of thin films of **1b** of various thickness (25, 64, 100, 120 and 145 nm) were back-calculated. The calculated reflection spectra of the films of **1b** were quite similar to those measured (Fig. 4) of corresponding thickness. These observations revealed that the complex refractive index at a specific energy was not sensitive to the film thickness.

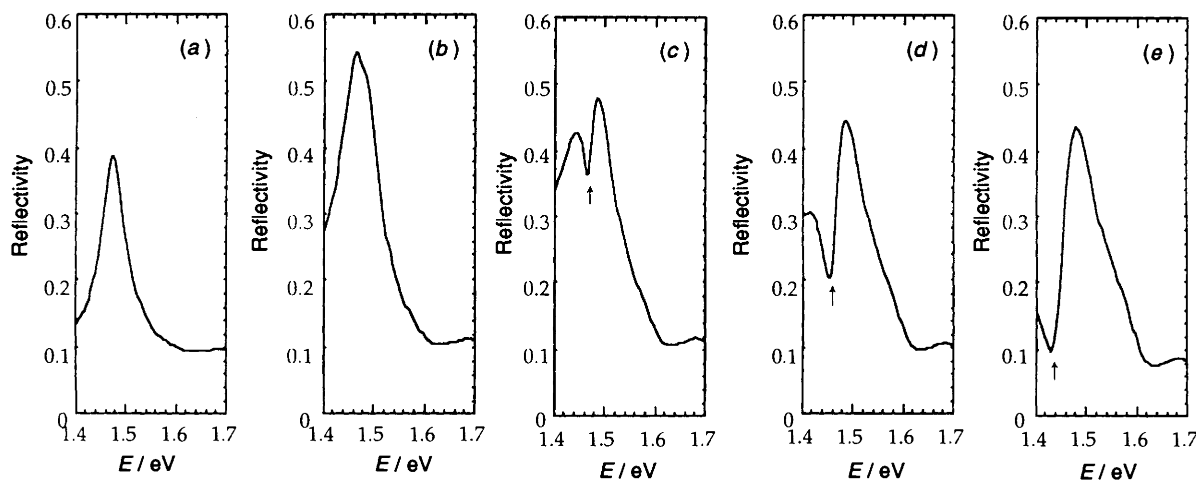

Fig. 4 Air-incident reflection spectra of thin films of **1b** of various thicknesses [thickness: (*a*) 25, (*b*) 64, (*c*) 100, (*d*) 120 and (*e*) 145 nm]. The ↑ sign shows the reflection spectral hole.

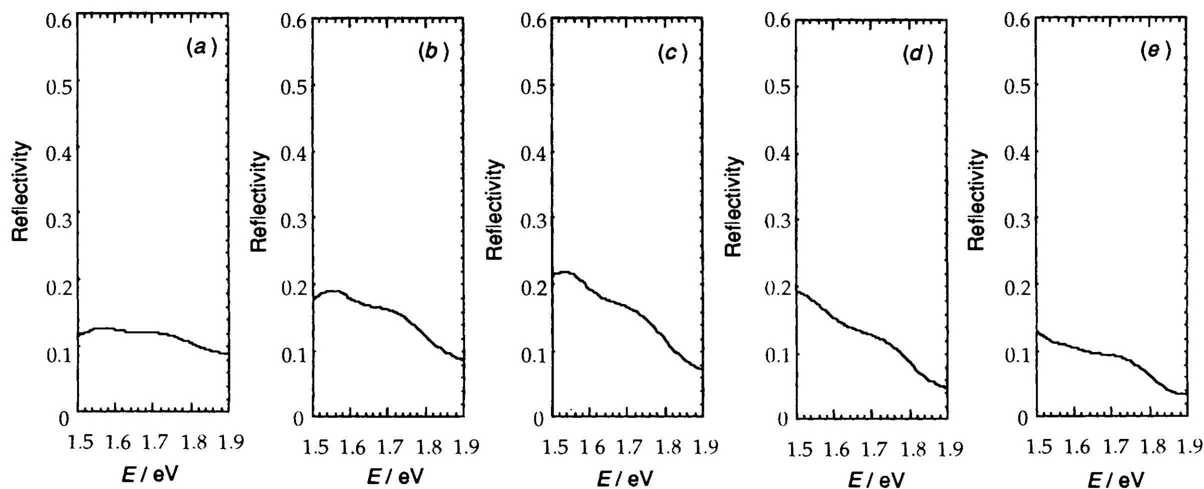

Fig. 5 Air-incident reflection spectra of thin films of **2a** of various thicknesses [thickness: (*a*) 20, (*b*) 60, (*c*) 90, (*d*) 120 and (*e*) 150 nm]

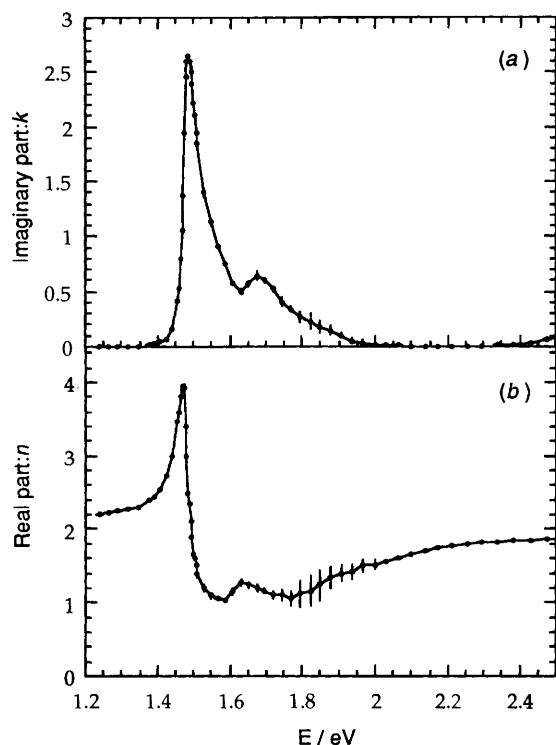

Fig. 6 Action spectra of imaginary [k: (a)] and real parts [n: (b)] of the complex refractive index of a thin film of **1b**, including error bars

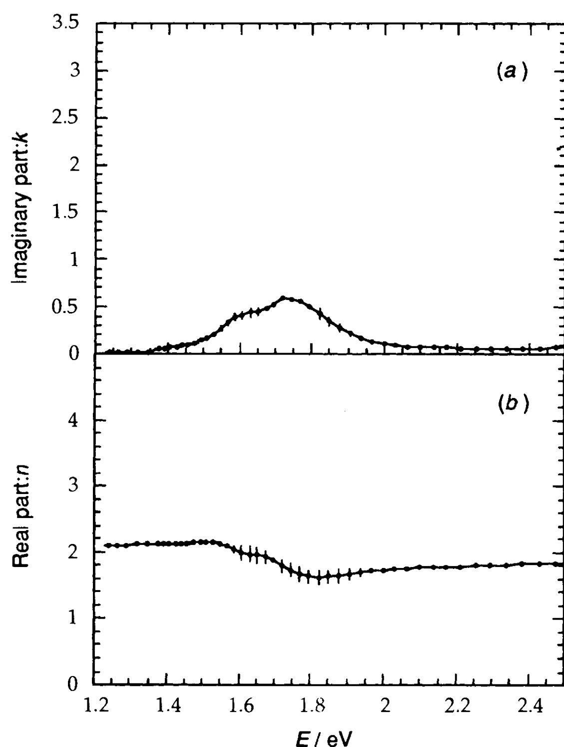

Fig. 7 Action spectra of imaginary [k: (a)], and real parts [n: (b)] of the complex refractive index of a thin film of **2a** including error bars

There were two maxima of k in the near IR region. The maximal k-value at 1.49 eV was over 2.5 and the other at 1.67 eV was 0.6. Below 1.47 eV, the n-value increased with k. A large maximal n-value (3.95) was observed at 1.47 eV, which was slightly lower than the energy of the k-maximum (1.49 eV). The energy relationship between the n- and k- maxima can be explained using the Kramers–Kronig relationship.[9] The high maximal n-value with strong dispersion at 1.47 eV has not been observed in any other dye. The n-value significantly decreased to about 1 above 1.47 eV. In contrast, the extremely broad action spectra of k and n of the film of **2a** compared with those of **1b** are shown in Fig. 7(a) and (b), respectively. Although there were two k-maxima around 1.60 and 1.74 eV, the maximal k-values were relatively low compared with that of **1b**.

The ε value was calculated from the n and k values described above using eqn. (17),[10] where ε_1 and ε_2 are real and imaginary parts of the complex dielectric constant, respectively.

$$\varepsilon = \varepsilon_1 - i\varepsilon_2 = n^2 - k^2 - i2nk \qquad (17)$$

The action spectra of the complex dielectric constants (ε_1 and ε_2) for thin films of **1b** and **2a** are shown in Fig. 8(a) and (b), respectively. The complex dielectric constant was further analysed using the harmonic oscillator model [Lorenzian model, eqn. (18)],[11] where E_j, S_j and γ_j are photon energy, relative

$$\varepsilon(E) = \sum_{j=1}^{\infty} \frac{S_j E_j^2}{E_j^2 - E^2 + i\gamma_j E} + C \qquad (18)$$

oscillator strength and band width of the j-th peak, respectively. C is a dielectric constant at a sufficiently high energy region. Parameters (E_j, S_j and γ_j) of the harmonic oscillator model were estimated by optimal fitting to the data of ε_2 depicted in Fig. 8 using eqn. (18). The action spectrum of ε for the film of **1b** was resolved into three peaks (P_1, P_2 and P_3) as shown in Fig. 8(a). In contrast, the action spectrum of ε for the film of **2a** showed featureless and broad peaks which were resolved into Q_1 and Q_2 as shown in Fig. 8(b). The parameters of each peak are summarized in Table 1. The largest peak (P_1) at 1.48 eV of the film of **1b** has an oscillator strength of 0.20 with a peak width of 0.018 eV. Two peaks (Q_1 and Q_2) at 1.60 and 1.74 eV of the film of **2a** have oscillator strengths of 0.08 and 0.24 with peak widths of 0.14 and 0.22 eV, respectively. Here P_1 was compared with Q_2, because P_1 and Q_2 having a similar oscillator strength were larger than the other peaks of thin films of **1b** and **2a**, respectively. The peak widths (γ) of P_1 and Q_2 were quite different. The peak width of P_1 for the film of **1b** was 1/7 less than that of Q_2 for the film of **2a**. Thus, the sharp dielectric maximum of the film of **1b** with a large oscillator strength and a narrow peak width might cause the high reflectivity. To clarify the influence of the peak width (γ) of the dielectric maximum on the reflectivity, the reflection spectra of model thin films of a 40 nm thickness when γ = 0.02, 0.05 and 0.10 eV were calculated using eqns. (17) and (18) as well as assuming a constant oscillator strength of 0.30 around 1.60 eV. As shown in Fig. 9, when the γ-value of a dielectric maximum with a constant oscillator strength was decreased, the maximal reflectivity significantly increased together with the maximal k- and n-values. Therefore, these analyses of the complex dielectric constant showed that a sharp dielectric maximum of the thin film of **1b** with a large oscillator strength and a narrow peak width induced high reflectivity, large k-maxima with a narrow width and large n-maxima with a strong dispersion.

From the energy relationship between the n- and k-maxima due to the sharp dielectric maximum of the film of **1b**, an energy region with large n (3.20) and small k (0.285) appeared at 1.45 eV, which was close to 1.49 eV with large n (2.50) and large k (2.65). The dependence of the calculated reflectivity upon the thickness of the film of **1b** at 1.45 and 1.49 eV are shown in Fig. 10. At 1.45 eV [Fig. 10(a): λ = 855 nm; n = 3.20 and k = 0.28], when the optical path difference (2 × thickness × n of the film) of two beams reflected from between the air/film and the film/glass interfaces is $\lambda/2$ (427 nm), these beams are in phase. In contrast, the two beams are out of phase when the optical path difference of the reflected beams is in integral multiples of λ (0, 855 nm). From interference between these beams, the reflectivity maximum was around 65 nm, while the

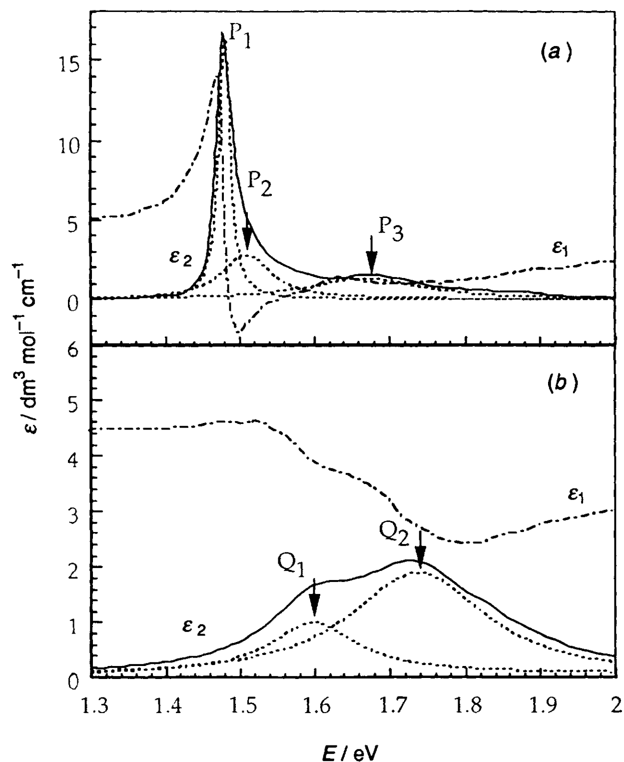

Fig. 8 Action spectra of imaginary (ε_2: —) and real parts (ε_1: – • –) of the complex dielectric constant of **1b** (*a*) and **2a** (*b*) thin films. Dotted lines (- - -) show resolved action spectra of their imaginary parts (ε_2).

Table 1 Parameters (S_j, E_j and γ_j) of the harmonic oscillator model for thin films of **1b** and **2a**

	Peak	S_j	E_j/eV	γ_j/eV
1b	P_1	0.20	1.48	0.018
	P_2	0.15	1.51	0.080
	P_3	0.14	1.67	0.18
2a	Q_1	0.08	1.60	0.14
	Q_2	0.24	1.74	0.22

reflectivity minima were around 0 and 130 nm thickness as shown in Fig. 10(*a*). On the contrary, at 1.49 eV [Fig. 10(*b*): λ = 832 nm; n = 2.50 and k = 2.65], the influence of the beam reflected from the film/glass interface decreased with increasing the film thickness due to the large k-value (2.65). By decreasing this influence, although reflectivity dependence on the film thickness was similar to that at 1.45 eV below 70 nm, the reflectivity at over 70 nm was almost constant as depicted in Fig. 10(*b*). The significantly different dependence of reflectivity on film thickness over 70 nm generated a reflectivity drop around 1.45 eV from the almost constant level at 1.49 eV. Consequently, the reflectivity drop, which also arose from the sharp dielectric maximum of the **1b** film, induced the unique reflection spectral hole.

Similar results were obtained from analysing the complex dielectric constants of other **1** and **2** thin films.

Reflection spectra of thin films of **1a–d** are shown in Fig. 11. Their reflectivity maxima showed a red-shift upon decreasing the steric hindrance of the two Y groups (**1d**⇒**1c**⇒**1b**⇒**1a**). This result clearly indicates that reflection properties of thin films of **1** are significantly affected by a relatively ordered intermolecular interaction between molecules of **1**. As described previously,[5] their absorption properties were also influenced by the ordered intermolecular interaction. From analysing the intermolecular interaction using exciton model,[12] a slipped J-type molecular arrangement in a thin film of **1** generated the

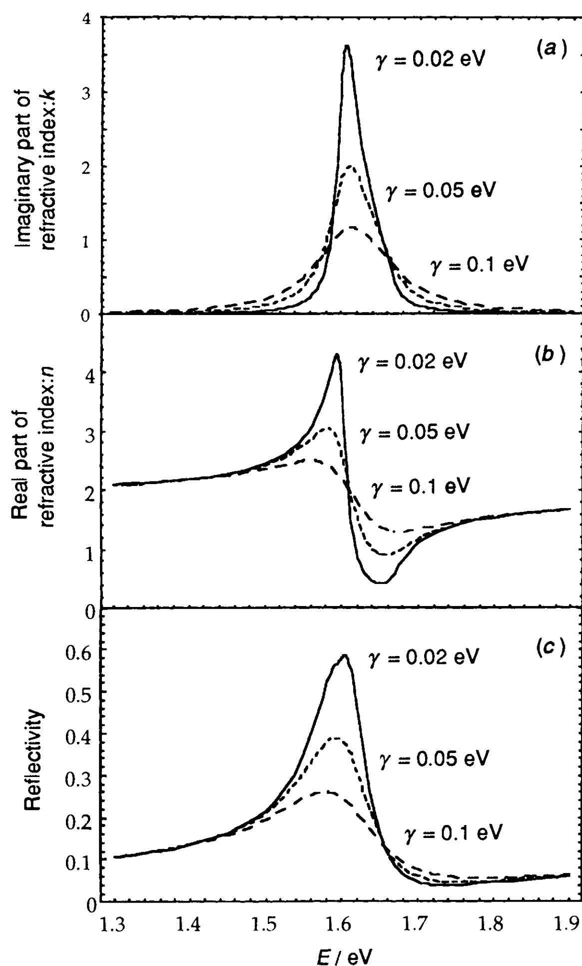

Fig. 9 Calculated action spectra of k (*a*), n (*b*) and reflectivity (*c*) of model thin films of a 40 nm thickness when γ = 0.02, 0.05 and 0.10 assuming E = 1.60 eV, S = 0.30 and C = 3.5

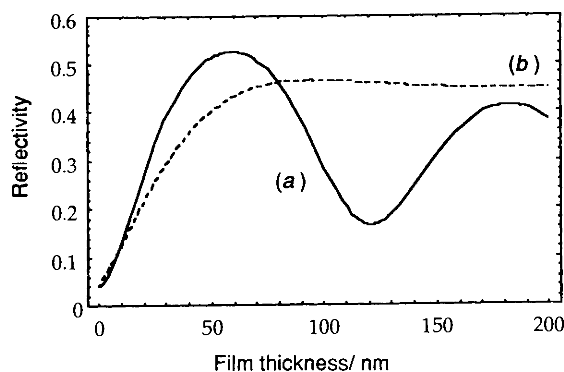

Fig. 10 Calculated reflectivity dependence on the thickness of a thin film of **1b** at 1.45 [(*a*): (—)] and 1.49 eV [(*b*): (- - -)]

ordered intermolecular interaction. The sharp dielectric maximum with a large oscillator strength and a narrow peak width should arise from the ordered intermolecular interaction. In contrast, a thin film of **2** consisted of a mixture of many H-type aggregates and a small amount of J-type arrangements because of their strong aggregating tendencies and the partial steric hindrance of the four X groups.[4] The complex and disordered molecular arrangement of a thin film of **2** caused the featureless and broad dielectric maximum with a wide peak width. Consequently, these different properties of the complex dielectric constants between thin films of Y_2MNcX_4 **1** and $MNcX_4$ **2** arose from their arrangements in thin films.

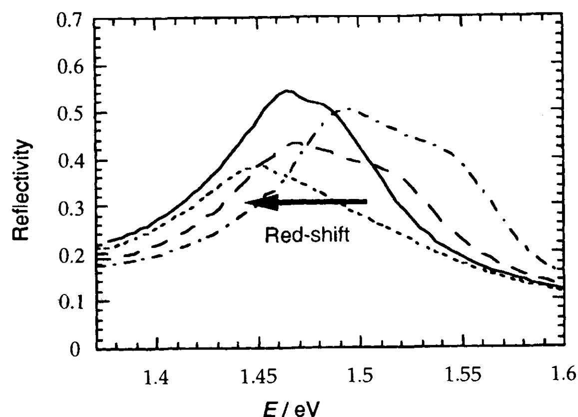

Fig. 11 Air-incident reflection spectra of thin films of **1a** (- - -), **1b** (—), **1c** (— — —) and **1d** (— · —) (thickness: **1a** 51, **1b** 64, **1c** 48 and **1d** 39 nm)

Conclusions

Using the observed transmission and reflection spectra of thin films of **1** and **2**, their complex dielectric constants were determined. An analysis of the complex dielectric constants showed that the high reflectivity of a thin film of **1** arose from its sharp dielectric maximum with a large oscillator strength and a narrow peak width. The sharp dielectric maximum should result from the ordered J-type molecular arrangement of the thin film of **1**. On the contrary, the low reflectivity of a thin film of **2** arose from a broad dielectric maximum with a wide peak width due to its complex and disordered molecular aggregation.

Acknowledgements

The authors wish to thank Dr Itsuo Watanabe, Mr Atsushi Kuwano and Dr Mitsuo Yamada in the Tsukuba Research Laboratory, Hitachi Chemical Co., Ltd., for their helpful suggestions.

References

1 (*a*) M. Hanack, G. Renz, J. Strahre and S. Schmid, *Chem. Ber.*, 1988, **121**, 1479; (*b*) M. Hanack, S. Deger, U. Keppeler, A. Lange, A. Leverenz and M. Rein, *Conducting Polymers*, 1987, 173; (*c*) M. Hanack, A. Lange, M. Rein, R. Behnisch, G. Renz and A. Leverenz, *Synth. Met.*, 1989, **29**, F1; (*d*) N. Q. Wang, Y. M. Cai, J. R. Hefflin and A. F. Garito, *Mol. Cryst. Liq. Cryst.*, 1990, **189**, 39; (*e*) A. F. Garito and J. W. Wu, *Proc. SPIE*, 1989, **1147**, 2; (*f*) L. Q. Minh, T. Chot, N. N. Dinh, N. N. Xuan, N. T. Binh, D. M. Phuoc and N. T. Binh, *Phys. Status Solidi*, 1987, **101**, K 143.

2 (*a*) H. Oba, M. Abe, M. Umehara, T. Sato, Y. Ueda and M. Kunikane, *Appl. Opt.*, 1986, **25**, 4023; (*b*) D. E. Nikeles, K. Chiang, H. A. Goldberg, R. S. Kohn and F. J. Onorato, *Proc. SPIE*, 1990, **1248**, 65; (*c*) T. Tomiyama, I. Watanabe, A. Kuwano, M. Habiro, N. Takane and M. Yamada, *Appl. Opt.*, 1995, **34**, 820.

3 S. Tai, M. Katayose and N. Hayashi, *Progr. Org. Coating*, 1994, **26**, 323.

4 S. Tai and N. Hayashi, *J. Chem. Soc., Perkin Trans. 2*, 1991, 1275.

5 M. Katayose, S. Tai, K. Kamijima, H. Hagiwara and N. Hayashi, *J. Chem. Soc., Perkin Trans. 2*, 1992, 403.

6 S. Tai, S. Hayashida and N. Hayashi, *J. Chem. Soc., Perkin Trans. 2*, 1991, 1637.

7 O. S. Heavens, *Optical Properties of Thin Solid Films*, Dover Publ., New York, 1991, p. 55.

8 (*a*) T. Fritz, J. Hahn and H. Bottcher, *Thin Solid Films*, 1989, **170**, 249; (*b*) T. C. Paulick, *Appl. Opt.*, 1986, **25**, 562; (*c*) R. D. Bringans, *J. Phys. D: Appl. Phys.*, 1977, **10**, 1855; (*d*) A. Hjorsberg, *Appl. Opt.*, 1981, **20**, 1254; (*e*) R. C. McPhedran, L. C. Botten, D. R. Mckenzie and R. P. Netterfield, *Appl. Opt.*, 1984, **23**, 1197.

9 P. N. Prasad and D. J. Williams, *Introduction to Nonlinear Optical Effects in Molecules and Polymers*, Wiley, Chichester, 1991, p. 189.

10 L. Ward, *The Optical Constants of Bulk Materials and Films*, Adam Hilger, Bristol, 1988, p. 9.

11 R. W. Ditchburn, *Light*, Dover, New York, 1991, p. 459.

12 (*a*) M. Kasha, M. A. El-bayoumi and W. Rhodes, *J. Chem. Phys.*, 1961, **58**, 916; (*b*) M. Kasha, H. R. Rawls and M. A. El-bayoumi, *Pure Appl. Chem.*, 1965, **11**, 371; (*c*) M. Kasha, *Radiation Research*, 1963, **20**, 55.

Paper 5/04434K
Received 6th *July* 1995
Accepted 8th *January* 1996